Food Packaging and Shelf Life 23 (2020) 100462

Contents lists available at ScienceDirect

Food Packaging and Shelf Life

journal homepage: www.elsevier.com/locate/fpsl

Fabrication of antimicrobial films based on hydroxyethylcellulose and ZnO for food packaging application

Gomaa El Fawal[a,c], Huoyan Hong[a], Xinran Song[a], Jinglei Wu[a], Meiqi Sun[a], Chuanglong He[a], Xiumei Mo[a], Yuxin Jiang[b,*], Hongsheng Wang[a,*]

[a] Key Laboratory of Science & Technology of Eco-Textile, Ministry of Education, College of Chemistry, Chemical Engineering and Biotechnology, Donghua University, Shanghai, 201620, China
[b] Department of Pathogenic Biology and Immunology, School of Medicine, Jiaxing University, Jiaxing, 314001, China
[c] Polymer Materials Research Department, Advanced Technology and New Materials Research Institute, Scientific Research and Technological Applications City (SRTA-City), New Borg El-Arab City, Alexandria, 21934, Egypt

ARTICLE INFO

Keywords:
Hydroxyethylcellulose (HEC)
Zinc oxide
Food packaging
Antimicrobial

ABSTRACT

The study aims to prepare antimicrobial films for food packaging using hydroxyethylcellulose (HEC) biopolymer to decrease environmental problems of synthetic polymer. Different ZnO concentrations (0.05, 0.1, and 0.2 %) were incorporated into HEC. The citric acid (CA) was used as a crosslinker for HEC and the casting method was used to prepare HEC/CA and HEC/CA/ZnO films. The prepared films were characterized by FT-IR, XRD, TGA and SEM. Also, mechanical, wettability and antimicrobial properties were examined. The presence of ZnO particles in the films was confirmed by XRD. SEM showed surface morphological differences between HEC/CA and HEC/CA/ZnO films. HEC/CA/ZnO film inhibited the growth of *Staphylococcus aureus* (91.4 %) and *Escherichia coli* (61.7 %) bacteria. Consequently, the prepared films consider a promising material for food packaging application.

1. Introduction

Recently, there is an increasing interest for films based on natural polymers, as they proved a wide range of applications (Hamid, Abolfazl, Ali, Marija, & Seyran, 2019; Shiv, Long-Feng, & Jong-Whan, 2019). The application of biopolymers in food packaging as an alternative to synthetic polymers has increased due to its degradability, availability, biocompatibility, relatively low cost, and nontoxicity (Kanatt & Makwana, 2020; Shiv et al., 2019). Some natural polymers have been used for packaging films like carrageenan, chitosan, alginate, and starch (El-Fawal, 2014; Tabassum & Khan, 2020; Wang, Lim, Tong, & Thian, 2019). Polysaccharides are attractive biopolymers owing to their good colloidal nature, film-forming ability, reasonable gas barrier and mechanical strength properties (Yu, Shen, Song, & Xie, 2018; Zeng, Li, Chen, & Zhang, 2019). Also, it has many biological activities, like antitumor (Xie et al., 2020), antioxidant (Ji et al., 2019, Mirzadeh, Arianejad, & Khedmat, 2020), antibacterial (Mirzadeh et al., 2020), hepatoprotective (Wang, Luo, Chen, Zha, & Pan, 2015), immunological activities (Li et al., 2017), and anti-inflammatory (Zhang, Pan, Ran, & Wang, 2019). But, film properties and antimicrobial activity of those polysaccharide-based films depend on the type of polysaccharide and active antimicrobial agent used (Kanmani & Rhim, 2014). Hydroxyethylcellulose (HCE) is one of the significant cellulosic ether derivatives and approved by the U.S. Food and Drug Administration (FDA). Owing to its low toxicity, non-immunogenicity and biocompatibility, it was used as thickener or binder, or as a protective suspension and colloid stabilizer in many applications, such as coating, biomedical and food applications (Aqdas et al., 2019; Kanmani & Rhim, 2014). For example, HEC with silver nanoparticle was used as a scaffold for skin tissue engineering applications (Zulkifli, Hussain, Zeyohannes, Rasad, & Yusuff, 2017). Also, HEC with hyaluronic acid was used as a wound dressing material (Pengfeng, Liangling, Wenyan, Lihong, & Min, 2018).

Nanofillers are additives in solid form (nanoparticles), which differ from the polymer matrix in terms of their composition and structure with particle sizes in the 1–100 nm range (Poole & Owens, 2003). Some of these nanoparticles (e.g., ZnO, Fe_3O_4, Ag, and TiO_2,) possess good stability, hydrophilicity, nontoxicity, and low cost (Mittal, 2016). Nanofillers play two roles in polymer blends. The first is the enhancement of several properties such as barrier, mechanical, thermal, and electrical properties. The second is the modification of miscibility/compatibility and morphology of polymer blends (Roberto & Luigi, 2014; Yoksan & Chirachanchai, 2010). When nanofillers were added to suitable

* Corresponding authors.
E-mail addresses: jiangyuxin2000@hotmail.com (Y. Jiang), whs@dhu.edu.cn (H. Wang).

https://doi.org/10.1016/j.fpsl.2020.100462
Received 20 October 2019; Received in revised form 29 December 2019; Accepted 2 January 2020

polymer matrix, they can be used in different applications such as separation and purification (Ahmed, Marcel, Ahmed, & Mathias, 2019), biomedicine (Ghassane et al., 2019), and food packaging (Olusola, Sisanda, Freeman, Williams, & Peter, 2019; Raghunath & Perumal, 2017). Zinc oxide - one of the nanofillers - is attractive in the food packaging industry because it has a wide spectrum of antimicrobial property (Maharubin et al., 2019). The Food and Drug Administration has recorded ZnO as safe substance (GRAS). ZnO has been added to various polymers to produce antimicrobial food packaging materials. For example, Ahmed, Mulla et al. (2019) incorporated (ZnO) nanoparticles into polylactide/polyethylene glycol/polycaprolactone and they found that the composite showed excellent antibacterial activity. Thi, Thi, Thi, and Pornchai, (2018)) prepared nanocomposite film through a combination of pectin/alginate and ZnO and they found that the film presented a potential application as edible films. These studies confirmed that the addition of ZnO could enhance the antibacterial performance of the film.

This study aims to prepare antimicrobial films using HEC biopolymers with nanofillers (ZnO) to get bio-based film for food packaging application, consequently decrease the environmental problems of the synthetic polymer. The films were characterized by Fourier transform infrared spectroscopy (FT-IR), X-Ray diffraction (XRD), and Scanning electron microscope (SEM) analysis. Besides, mechanical and wettability properties were examined. The films antimicrobial activity was tested against Gram-positive *Staphylococcus aureus* (*S. aureus*) and Gram-negative *Escherichia coli* (*E. coli*) bacteria.

2. Material and methods

2.1. Material

Hydroxyethylcellulose (Mw = 250,000), citric acid (monohydrate), ZnO (dispersion, nanoparticles < 100 nm particle size), and Luria-Bertani medium (LB) were purchased from Sigma Aldrich, China. All the chemicals were used without further purification.

2.2. Methods

2.2.1. Hydroxyethylcellulose film preparation

Casting method was used for HEC/CA and HEC/CA/Zn films preparation. The HEC (2 g) was dissolved in 100 mL distilled water and stirred continuously for 1 h at 70 °C till HEC completely dissolved. The citric acid (CA) (25 % w/w) was added to HEC as a crosslinker with stirring for 2 h at 70 °C – in this case we get HEC/CA blank film. After that, ZnO (0.05, 0.1, and 0.2 %) was added to the solution with stirring for 1 h at 70 °C – in this case we get HEC/CA/Zn films. Finally, 25 mL of the solution were transferred to a Petri dish for drying (overnight, 70 °C). Then the films underwent heat treatment at 110 °C for 10 min. for the crosslinking step. The films were kept in vacuum oven till used.

2.3. Characterization

2.3.1. Fourier transform infrared spectroscopy (FT-IR) analysis

Fourier transform infrared spectroscopy (FT-IR) (Nicolet 6700, Thermo Fisher, USA) was used to record the IR spectra of HEC, HEC/CA and HEC/CA/ZnO films. Sixteen scans were collected with a 4 cm^{-1} resolution for all spectra.

2.3.2. X-ray diffraction (XRD) analysis

Shimadzu X-ray diffraction (XRD) (7000, USA, Cu-Kα radiation) was used to confirm the presence of ZnO at 1.5406 Å wavelength and step size 20. The data were collected in the range of $10 \leq 2\theta \leq 60^{\circ}$ - in the form of 2θ versus intensity (a.u) chart. ZnO and HEC/CA/ZnO films had undergone heat treatment at 300 °C for 5 min. before using the X-ray diffraction device.

2.3.3. Morphology of hydrogel membrane

Scanning electron microscope (SEM, Hitachi TM-100, Japan) was used to observe film morphology (surface and cross-section). The films were coated with gold before imaging (two times for 45 s).

2.3.4. Gel fraction determination

This method used to check the crosslinking process efficiency by determining the gel content percentage. The gel content of a given material was calculated by measuring the insoluble parts of a dried sample after immersion in a solvent, while the non-crosslinked fraction was dissolved and migrated to the solvent (Francis, Mitra, Dhanawade, Varshney, & Sabharwal, 2009). The HEC/CA and HEC/CA/ZnO films were dried in an oven for 6 h at 60 °C to the weight, W_0. After that, the films were soaked in distilled water for 24 h at 37 °C (for elimination the soluble parts from the films). Finally, the films were dried in an oven for 10 h at 60 °C to weight, W_1. The gel fraction (GF %) was calculated by

$$\text{Gel fraction (GF \%)} = [W_1/W_0] \times 100\% \quad (1)$$

Tests were carried out in triplicate and were described as a mean value.

2.3.5. Swelling behavior

Material capacity to absorb solvents was determined via swelling test. The films were cut into 1 cm × 1 cm and dried at 60 °C in an oven for 10 h to weight, W_0. The dried films were soaked in distilled water and incubated at 37 °C. At certain time intervals, samples were weighted (W_t) after wiping off the excess surface water using filter paper. The water uptake was calculated by

$$\text{Water uptake (\%)} = \{[W_t - W_0]/W_0\} \times 100\% \quad (2)$$

where, W_t is the weight of swollen samples at a time, t and W_0 is the initial weight of samples. Tests were carried out in triplicate and were described as a mean value.

2.3.6. Mechanical properties

Universal materials testing machine (H5K-S, Hounsfield, UK) was used to examine the mechanical properties (tensile strength (TS) and elongation at break (E%)) - at room temperature. The cross-head speed was 10 mm/min. to test all specimens (10 mm × 50 mm, n = 3). The electronic digital micrometer (Mitutoyo, Japan) was used to measure specimen thickness. “E” expresses the percentage change of initial gauge length for the specimen (50 cm) at the point of its failure. “TS” was considered by dividing force (maximum load) by the initial cross-sectional area of a specimen. Tests were carried out in triplicate and were described as a mean value.

2.3.7. Antibacterial activity determination

ELIZA microplate reader assay was used to test films antimicrobial activity (Wang et al., 2010). Foodborne pathogens strain *S. aureus* (Gram-positive) and *E. coli* (Gram-negative) bacteria were obtained from the Institute of Biological Science and Engineering, Donghua University, China. LB broth medium was used to refresh the bacterial cells and incubated overnight at 37 °C. Aliquot of 500 µl of refresh bacterial strains (104 CFU/ml) was transferred to each well of 6-well plates. A square film (1 cm × 1 cm, sterilized with UV for 4 h) were added to each well in replica and incubated at 37 °C for one week. Finally, automated ELIZA microplate reader was used to determine the absorbances at 620 nm every day for one week.

The inhibition percentage was calculated by the equation:

$$\text{Inhibition percentage} = \{[A_0 - A_1]/ A_0\} \times 100\%$$

where, A_o is the absorbance of the control group and A_1 is the absorbance of the treated group

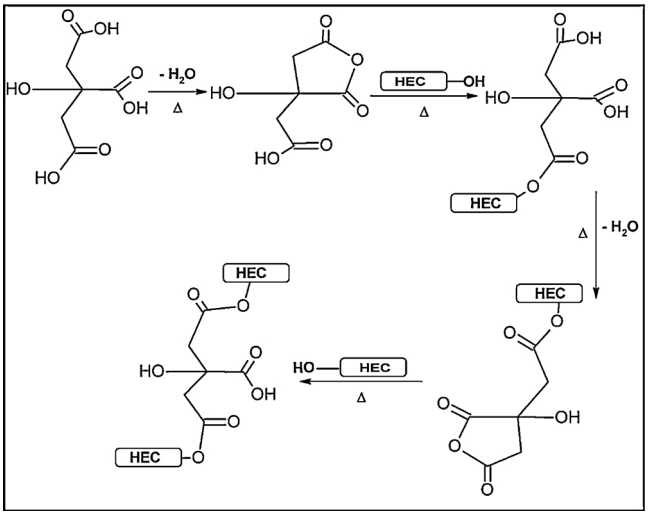

Scheme 1. Possible crosslinking reaction between HEC and CA (HEC: Hydroxyethylcellulose; CA: Citric acid).

2.3.8. Statistical analysis

All data were presented as mean ± standard deviation (SD) and the error bars in the figures are the SDs of the data. Obtained results were statistically analyzed by SPSS software (version 22.0; IBM Corp., Armonk, NY). All statistical analysis was used one-way analysis of variance (ANOVA). Probability values (p) of < 0.05 ($p < 0.05$) were interpreted as the occurrence is statistically significant at the 0.05 level.

3. Results and discussion

3.1. Hydroxyethylcellulose crosslinking reaction

The CA has been applied in drug and food applications as a preservative and crosslinking agent (Coma, Sebti, Pardon, Pichavant, & Deschamps, 2003; El Fawal, Abu-Serie, Hassan, & Elnouby, 2018; Ghorpade, Yadav, & Dias, 2017). Different mechanisms explain the crosslinking reaction between CA and HEC. The crosslinking reaction is based on the esterification reaction between hydroxyl groups (HEC) and carboxylic groups (CA) (Scheme 1). The esterification reaction depends on anhydride intermediate formation. Carboxylic groups (from CA) undergo dehydrates to form a cyclic anhydride - under heating- that combine with hydroxylic groups (form HEC). The residual carboxylic groups dehydrate to form other intra-molecular anhydrides which combine with other hydroxylic groups. The same behavior was found when CA was used as a crosslinker for hydroxypropyl methylcellulose (HPMC) (Coma et al., 2003).

3.2. Fourier transform infrared spectroscopy (FT-IR) analysis

The FT-IR spectrum for HEC/CA and HEC/CA/ZnO films has been showed over the wavenumber range 500–4000 cm^{-1} (Fig. 1). The FT-IR spectra for HEC (powder) show the characteristics bands for it (Table 1) (Sekiguchi, Sawatari, & Kondo, 2003; Vieira et al., 2009). HEC/CA film displays the same characteristic bands for HEC besides a band at 1654.9 cm^{-1} that represent the ester group band between HEC (O—H) and CA (C═O). The same behavior was observed when HEC crosslinked using CA (El Fawal et al., 2018). The FT-IR spectra for HEC/CA/ZnO films show that the ZnO has a small effect on the functional groups intensities of HEC/CA film as a result of the interactions between HEC/CA groups and ZnO. The absorbance for —OH group, at 3445.2 cm^{-1}, decreases and shifts to lower wavenumber (3315.5 cm^{-1}) and become broad with adding ZnO. The C═O absorption band shifts to a lower frequency owing to the hydrogen bond between the crosslinked HEC/CA and ZnO. The same behavior was

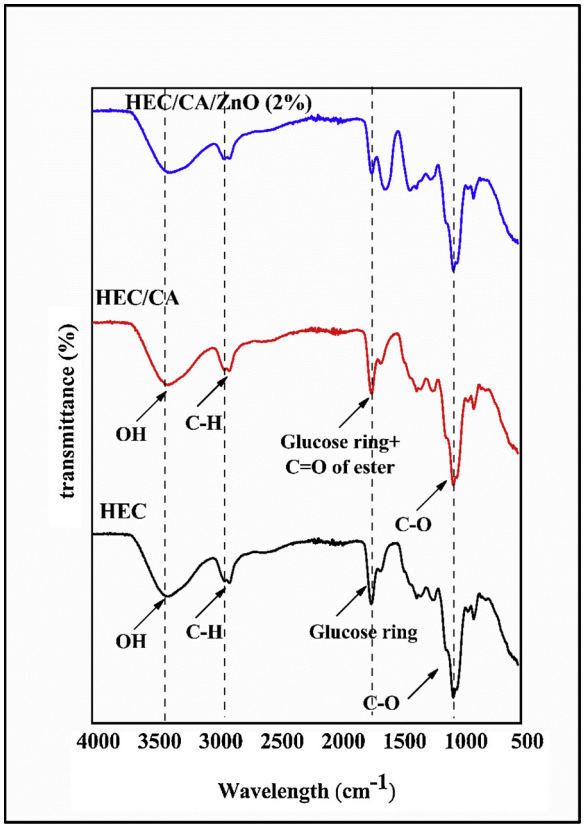

Fig. 1. FTIR spectra of HEC (powder), HEC/CA film, and HEC/CA/ZnO film (HEC: Hydroxyethylcellulose; CA: Citric acid; ZnO: Zinc oxide).

Table 1
Functional groups for HEC/CA film.

Wavelength (cm^{-1})	Assign group
3445.2	—OH group stretching of carboxylic group
2930.3	C—H of carboxylic group
1654.9	Glucose ring / COO^-
1085.4	C—O bond

observed when ZnO was added to polyvinyl alcohol/carboxymethyl cellulose film (Abutalib, 2019). Also, those results agree with work having used HEC as a reducing and stabilizing agent in the synthesis of stable silver nanoparticles (El-Sheikh, El-Rafie, Abdel-Halim, & El-Rafie, 2013). Comparing the FT-IR of HEC/CA and HEC/CA/ZnO films, it is clear that the position of OH and C—O stretching shift little. This is evidence for the formation of a hydrogen bond between ZnO and HEC/CA. The same behavior was observed after incorporation of the ZnO with chitosan (Kumar et al., 2012).

3.3. X-ray diffraction analysis

HEC/CA and HEC/CA/ZnO films X-ray patterns are shown in Fig. 2. The HEC/CA film has no diffraction peaks and this agrees with earlier XRD pattern of polysaccharides like carboxymethyl cellulose and carrageenan (Kanmani & Rhim, 2014). The HEC/CA/ZnO film shows characteristic diffraction peaks at 2 θ of 56.6, 47.6, 36.3, 34.5, and 31.8 which match to (110), (102), (101), (002), and (100) planes of ZnO, respectively (Tankhiwale & Bajpai, 2012). Similar results were reported when ZnO integrated with cellulose acetate and carboxymethyl cellulose (Anitha, Brabu, Thiruvadigal, Gopalakrishnan, & Natarajan, 2012; Ji et al., 2019; Yu, Yang, Liu, & Ma, 2009).

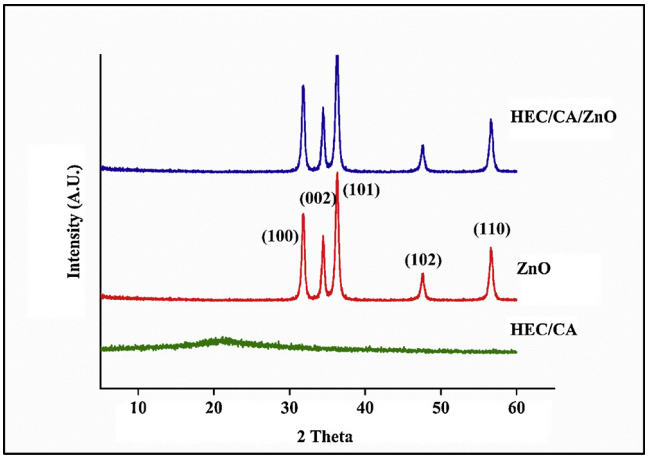

Fig. 2. X-ray diffraction (XRD) patterns of HEC/CA and HEC/CA/ZnO films (HEC: Hydroxyethylcellulose; CA: Citric acid; ZnO: Zinc oxide).

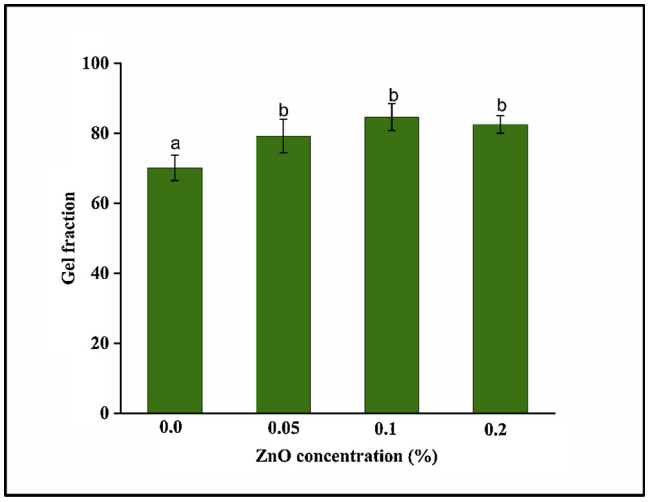

Fig. 4. Gel fraction of HEC/CA and HEC/CA/ZnO films (HEC: Hydroxyethylcellulose; CA: Citric acid; ZnO: Zinc oxide).

3.4. Morphology of the film

The HEC/CA film has fine morphology with a smooth surface (Fig. 3a). While HEC/CA/ZnO film displays rough surface structures with unequal and random distributed ZnO (Fig. 3b). It also shows the presence of aggregation and different shapes of ZnO. Similar results were reported when ZnO was added to polyurethane acrylate and polypropylene film (Kim et al., 2012; Paisoonsin, Pornsunthorntawee, & Rujiravanit, 2013).

3.5. Gel fraction determination

Gel fraction content is the dried film parts after soaking in water. The gel fraction percentage of HEC/CA film is 70.1 %, and it increases to be 79.2 % by using ZnO (0.05 %) (Fig. 4). Increasing ZnO concentration more than 0.05 % shows an insignificant effect on gel fraction percentage. These results demonstrate that the addition of ZnO to HEC/CA film improves the cross-linking network and increases the insolubility part in water. These results agree with earlier work which stated that the film can be cross-linked with ions (multivalent), e.g., W^{2+} and Al^{3+} due to their ability to form chelation with the hydroxyl groups (Ninan et al., 2013; Yang, Zhang, Peng, & Zhong, 2000). But our results are incompatible with the work of Tingting et al. (2019) when they used ZnO with sodium alginate and they found that the gel fraction decreased as ZnO concentrations increased.

3.6. Swelling behavior

Film water uptake percentage plays a vital role in expecting the film

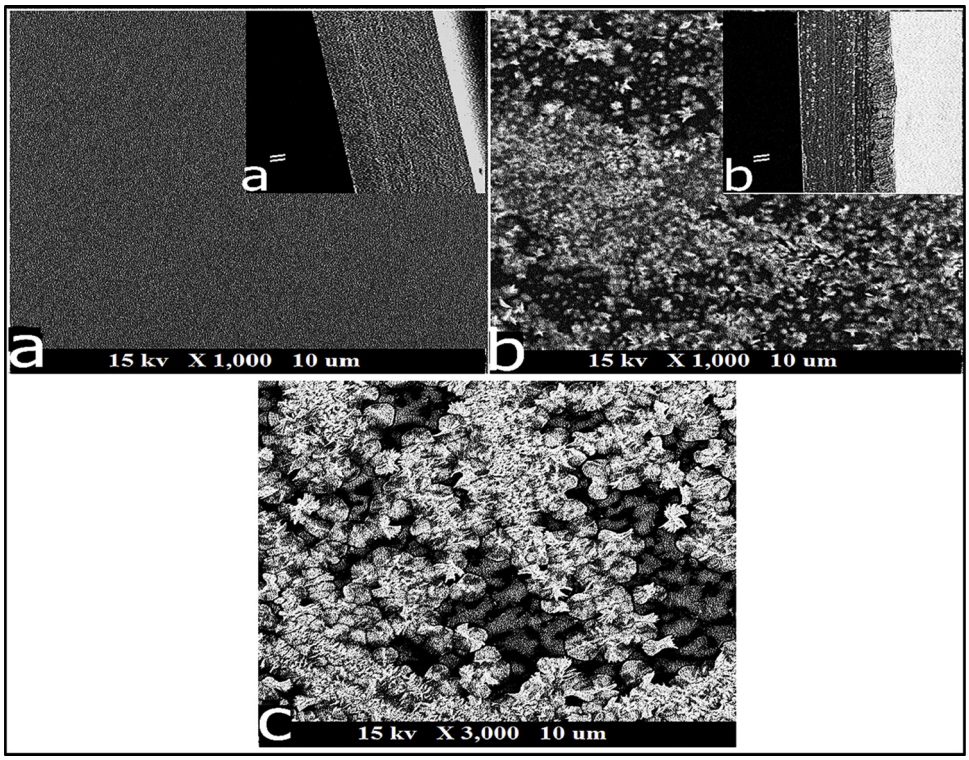

Fig. 3. SEM micrograph of the HEC/CA [a: surface; a': cross-section] and HEC/CA/ZnO [b: surface; b': cross-section; and c: surface] films. White color indicates the distribution of ZnO (HEC: Hydroxyethylcellulose; CA: Citric acid; ZnO: Zinc oxide).

Table 2
Water uptake percentage of HEC/CA and HEC/CA/ZnO films.

Time (h)	ZnO concentration (%)			
	0	0.05 %	0.1 %	0.2 %
2	138 ± 15[a]	190 ± 12[b]	150 ± 13[a]	97.9 ± 13[c]
4	160.8 ± 15[a]	242.7 ± 19[b]	219.1 ± 16[b]	136.7 ± 15[c]
8	176.9 ± 24[a]	272.7 ± 24[b]	241.8 ± 20[b]	149.8 ± 10[c]
24	193.1 ± 20[a]	307.3 ± 27[b]	277.3 ± 23[c]	159.2 ± 11[d]
48	206.1 ± 27 [a]	354.5 ± 18[b]	315.1 ± 19 [b]	160.2 ± 13 [c]
72	210.8 ± 22 [a]	359.2 ± 15[b]	326.4 ± 17 [b]	162.2 ± 17 [c]
168 (week)	213.3 ± 24 [a]	362.1 ± 31[b]	324.5 ± 22 [b]	165.4 ± 12 [c]

*The analysis was done at a fixed time with the change in ZnO concentrations.

suitability for a specific application. Films behave like sponge porous material after 2 h, it has a high degree of water uptake (Table 2). The presence of strong hydrogen bonding between HEC/CA film chains makes it has 138 % water uptake (van der Linden, Herber, Olthuis, & Bergveld, 2003). This strong interaction facilitates water absorption and swelling without being dissolved and the results agree with earlier work for HEC crosslinked using CA (Bajpai, Jadaun, & Tiwari, 2016; El Fawal et al., 2018). Due to the presence of ZnO nanoparticles within the network that enhances the swelling percentage by interacting with water molecules, we found that the film containing ZnO (0.05 %) shows a high-water uptake (Bajpai et al., 2016). The swelling percentage decreases as ZnO concentration increases because ZnO makes more bonding with carboxyl groups and this leads to decrease in the free carboxyl groups for water molecules. These results agree with the work of Tingting et al. (2019) when used ZnO with sodium alginate and they found that ZnO effect on the swelling behavior of the films. Also, the results agree with work of Zulkifli et al. when used silver nanoparticle with HEC to prepare scaffolds for skin tissue engineering applications (Zulkifli et al., 2017).

3.7. Mechanical properties

Fig. 5 shows the effect of ZnO on the mechanical properties of HEC/CA and HEC/CA/ZnO films. The effect depends on the density and distribution of intra and intermolecular interactions among the polymer chains (Chambi & Grosso, 2006). The thickness of HEC/CA film is 24 ± 2 μm and it increases by 29.2 % after formation HEC/CA/ZnO film (0.2 %). A similar result was observed by Kanmani and Rhim (2014) for carrageenan and carboxymethylcellulose films, the thickness increased with the addition of ZnO. Also, a similar result was reported

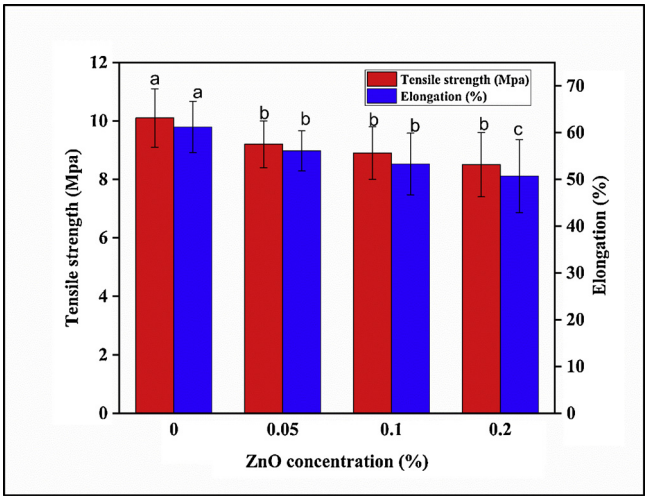

Fig. 5. Mechanical properties of HEC/CA and HEC/CA/ZnO films (HEC: Hydroxyethylcellulose; CA: Citric acid; ZnO: Zinc oxide).

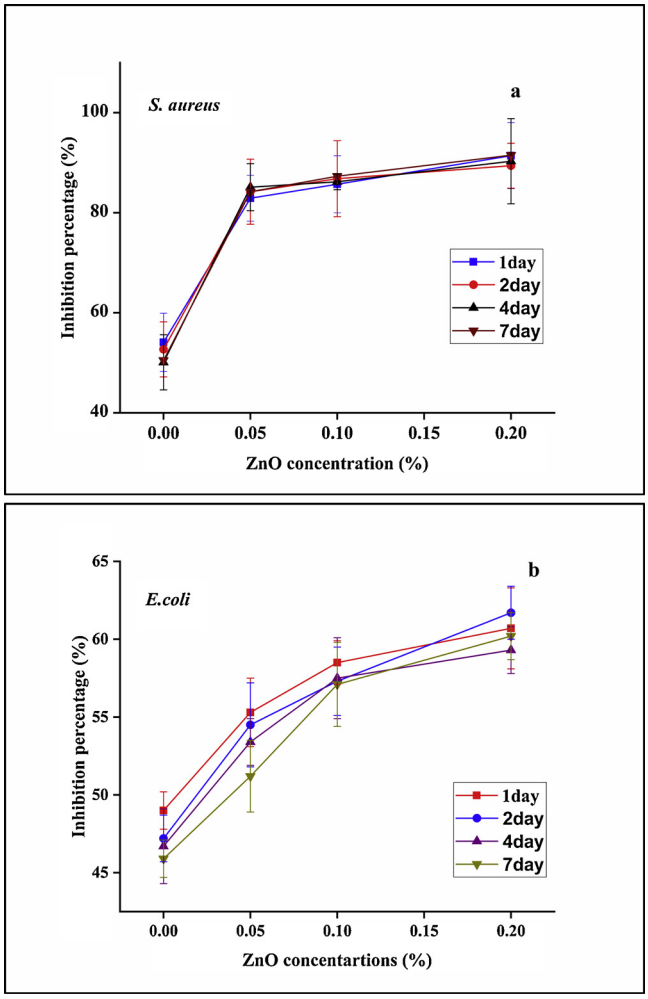

Fig. 6. Antibacterial activities of the HEC/CA and HEC/CA/ZnO films against *S. aureus* (a) and *E. coli* (b) (HEC: Hydroxyethylcellulose; CA: Citric acid; ZnO: Zinc oxide).

for poly(vinyl chloride) (PVC) films with ZnO NPs (Li, Xing, Li, Jiang, & Ding, 2010). When ZnO concentration increases from 0.05 to 0.2 %, the tensile strength decreases from 10.1–8.5 MPa. The decrease in mechanical properties with increasing ZnO refer to agglomeration, recrystallization, and non-uniform distribution of ZnO in the HEC/CA/ZnO film. These factors cause weak interfacial interaction between ZnO and HEC/CA matrix and cause decrease for mechanical properties. A similar result was reported earlier when ZnO was added to carboxymethyl cellulose and carrageenan (Oun & Rhim, 2017; Yu et al., 2009).

3.8. Antibacterial activity determination

Due to the presence of citric acid, HEC/CA film shows moderate inhibition percentage against *S. aureus* and *E. coli* strains (Fig. 6a, b). Earlier results were reported using citric acids to inhibit *E. coli* and *S. aureus* (Al-Rousan et al., 2018). But the inhibition percentage increases when ZnO was used, especially with *S. aureus* from 50.5 % to 91.5 % and for *E. coli* from 45.9 % to 60.2 % (after one week). The results confirm that ZnO is less effective against Gram-negative (*E. coli*) than Gram-positive (*S. aureus*) strains. The inhibition percentage against *S. aureus* and *E. coli* is high even after one week. Those results agree with earlier work of Anitha et al. (2012) and Nafchi, Alias, Mahmud, and Robal (2012) when they incorporated ZnO with cellulose acetate and sago starch. They found that ZnO was less effective against *E. coli* than

S. aureus strains. The ZnO antimicrobial activity depends on the bacterial cell wall structure. The cell wall structure of *E. coli* is complex with a fine peptidoglycan layer, while the cell wall structure of *S. aureus* is thick with many layers of peptidoglycan surrounded by an outer membrane (Anitha et al., 2012; Paisoonsin et al., 2013). In the case of *E. coli*, ZnO link with bacterial cell membrane that has phospholipids, lipopolysaccharide, and lipoprotein which decrease ZnO attachment (Anitha et al., 2012). But in case of *S. aureus*, ZnO link with a bacterial outer cell wall that has pores enough to facilitate ZnO penetration into the cells and therefore leads to intracellular contents leakage and the cell dies (Li, Feng et al., 2010). Many possible action mechanisms have been reported for ZnO antimicrobial activity. One of them supposes the highly reactive oxygen compounds generation like superoxide and hydroxyl radicals, peroxide ions, and hydrogen peroxide from ZnO surface (Li et al., 2009; Paisoonsin et al., 2013; Zhang et al., 2010). The hydroxyl and superoxide radicals - negatively charged- will stay in external bacteria cell wall membrane and damage the lipids, DNA, and proteins, whereas hydrogen peroxide can enter into the bacteria cell wall membrane and causes cell death (Paisoonsin et al., 2013; Tankhiwale & Bajpai, 2012; Zhang et al., 2010).

4. Conclusion

Different HEC/CA/ZnO films were prepared by a casting method using CA as a crosslinker. The XRD and SEM characterization suggests that ZnO was incorporated into HEC/CA film and the ZnO was distributed heterogeneous on the surface of the film. The wettability results indicated that HEC/CA/ZnO films have good swelling abilities and hydrophilicity. Also, the HEC/CA/ZnO films have good antibacterial properties and consequently, the films inhibited the growth of *S. aureus* (91.4 %) and *E. coli* (61.7 %) bacteria. In conclusion, the HEC/CA/ZnO film can be used as a promising antimicrobial packaging film.

Authors' contributions

All authors contributed equally

Declaration of Competing Interest

There is no Conflicts of interest

Acknowledgements

This research was supported by The National Key Research and Development Program of China (2018YFC1706200), Shanghai Science and Technology Committee Project (18490740400), National Natural Science Fund of China (81671586 and 31900949), and the Fundamental Research Funds for the Central Universities (2232019D3-20).

References

Abutalib, M. M. (2019). Effect of zinc oxide nanorods on the structural, thermal, dielectric and electrical properties of polyvinyl alcohol/carboxymethyle cellulose composites. *Physica B, Condensed Matter, 557*, 108–116.

Ahmed, J., Mulla, M., Jacob, H., Luciano, G., Bini, T. B., & Almusallam, A. (2019). Polylactide/poly(ε-caprolactone)/zinc oxide/clove essential oil composite antimicrobial films for scrambled egg packaging. *Food Packaging and Shelf Life, 21*, 100355.

Ahmed, M. A., Marcel, M., Ahmed, S. G., & Mathias, U. (2019). Nanofillers dissolution as a crucial challenge for the performance stability of thin-film nanocomposite desalination membranes. *Separation and Purification Technology, 228*, 115767.

Al-Rousan, W. M., Olaimat, A. N., Osaili, T. M., Al-Nabulsi, A. A., Ajo, R. Y., & Holley, R. A. (2018). Use of acetic and citric acids to inhibit Escherichia coli O157:H7, Salmonella typhimurium and Staphylococcus aureus in tabbouleh salad. *Food Microbiology, 73*, 61–66.

Anitha, S., Brabu, B., Thiruvadigal, D. J., Gopalakrishnan, C., & Natarajan, T. S. (2012). Optical, bactericidal and water repellent properties of electrospun nano-composite membranes of cellulose acetate and ZnO. *Carbohydrate Polymers, 87*(2), 1065–1072.

Aqdas, N., Khalid, M. Z., Shazia, T., Waseem, A., Muhammad, S., & Mohammad, Z. (2019). Hydroxyethylcellulose-g-Poly(lactic acid) blended polyurethanes: Preparation, characterization and biological studies. *International Journal of Biological Macromolecules* In Press.

Bajpai, S. K., Jadaun, M., & Tiwari, S. (2016). Synthesis, characterization and antimicrobial applications of zinc oxide nanoparticles loaded gum acacia/poly(SA) hydrogels. *Carbohydrate Polymers, 153*, 60–65.

Chambi, H., & Grosso, C. (2006). Edible films produced with gelatin and casein cross-linked with transglutaminase. *Food Research International, 39*(4), 458–466.

Coma, V., Sebti, I., Pardon, P., Pichavant, F. H., & Deschamps, A. (2003). Film properties from crosslinking of cellulosic derivatives with a polyfunctional carboxylic acid. *Carbohydrate Polymers, 51*(3), 265–271.

El-Fawal, G. (2014). Preparation, characterization and antibacterial activity of biodegradable films prepared from carrageenan. *Journal of Food Science and Technology, 51*(9), 2234–2239.

El-Sheikh, M. A., El-Rafie, S. M., Abdel-Halim, E. S., & El-Rafie, M. H. (2013). Green synthesis of hydroxyethyl cellulose-stabilized silver nanoparticles. *Journal of Polymers, 2013*, 11.

El Fawal, G. F., Abu-Serie, M. M., Hassan, M. A., & Elnouby, M. S. (2018). Hydroxyethyl cellulose hydrogel for wound dressing: Fabrication, characterization and in vitro evaluation. *International Journal of Biological Macromolecules, 111*, 649–659.

Francis, S., Mitra, D., Dhanawade, B. R., Varshney, L., & Sabharwal, S. (2009). Gamma radiation synthesis of rapid swelling superporous polyacrylamide hydrogels. *Radiation Physics and Chemistry, 78*, 951–953.

Ghassane, T., Marya, R., Omar, M., Mustapha, A., Abdelfattah, M., Frederic, B., et al. (2019). Black phosphorus-based polyvinylidene fluoride nanocomposites: Synthesis, processing and characterization. *Composites Part B Engineering, 175*, 107165.

Ghorpade, V. S., Yadav, A. V., & Dias, R. J. (2017). Citric acid crosslinked β-cyclodextrin/carboxymethylcellulose hydrogel films for controlled delivery of poorly soluble drugs. *Carbohydrate Polymers, 164*, 339–348.

Hamid, M., Abolfazl, K., Ali, M., Marija, Z., & Seyran, F. (2019). Nanocomposite films with CMC, okra mucilage, and ZnO nanoparticles: Extending the shelf-life of chicken breast meat. *Food Packaging and Shelf Life, 21*, 100330.

Ji, Y.-H., Liao, A.-M., Huang, J.-H., Thakur, K., Li, X.-L., & Wei, Z.-J. (2019). Physicochemical and antioxidant potential of polysaccharides sequentially extracted from Amana edulis. *International Journal of Biological Macromolecules, 131*, 453–460.

Kanatt, S. R., & Makwana, S. H. (2020). Development of active, water-resistant carboxymethyl cellulose-poly vinyl alcohol-Aloe vera packaging film. *Carbohydrate Polymers, 227*, 115303.

Kanmani, P., & Rhim, J.-W. (2014). Properties and characterization of bionanocomposite films prepared with various biopolymers and ZnO nanoparticles. *Carbohydrate Polymers, 106*, 190–199.

Kim, D., Jeon, K., Lee, Y., Seo, J., Seo, K., Han, H., et al. (2012). Preparation and characterization of UV-cured polyurethane acrylate/ZnO nanocomposite films based on surface modified ZnO. *Progress in Organic Coatings, 74*(3), 435–442.

Kumar, P. T., Lakshmanan, V.-K., Anilkumar, T. V., Ramya, C., Reshmi, P., Unnikrishnan, A. G., et al. (2012). Flexible and microporous chitosan hydrogel /nano ZnO composite bandages for wound dressing: In vitro and in vivo evaluation. *ACS Applied Materials & Interfaces, 4*, 2618–2629.

Li, J. H., Hong, R. Y., Li, M. Y., Li, H. Z., Zheng, Y., & Ding, J. (2009). Effects of ZnO nanoparticles on the mechanical and antibacterial properties of polyurethane coatings. *Progress in Organic Coatings, 64*(4), 504–509.

Li, Q.-M., Wang, J.-F., Zha, X.-Q., Pan, L.-H., Zhang, H.-L., & Luo, J.-P. (2017). Structural characterization and immunomodulatory activity of a new polysaccharide from jellyfish. *Carbohydrate Polymers, 159*, 188–194.

Li, X.-F., Feng, X.-Q., Yang, S., Fu, G.-Q., Wang, T.-P., & Su, Z.-X. (2010). Chitosan kills Escherichia coli through damage to be of cell membrane mechanism. *Carbohydrate Polymers, 79*(3), 493–499.

Li, X., Xing, Y., Li, W., Jiang, Y., & Ding, Y. (2010). Antibacterial and physical properties of poly(vinyl chloride)-based film coated with ZnO nanoparticles. *Food Science and Technology International, 16*, 225–232.

Maharubin, S., Nayak, C., Phatak, O., Kurhade, A., Singh, M., Zhou, Y., et al. (2019). Polyvinylchloride coated with silver nanoparticles and zinc oxide nanowires for antimicrobial applications. *Materials Letters, 249*, 108–111.

Mirzadeh, M., Arianejad, M. R., & Khedmat, L. (2020). Antioxidant, antiradical, and antimicrobial activities of polysaccharides obtained by microwave-assisted extraction method: A review. *Carbohydrate Polymers, 229*, 115421.

Mittal, V. (2016). *Spherical and fibrous filler composites.* Hoboken, NJ, USA: John Wiley & Sons 8, 138.

Nafchi, A. M., Alias, A. K., Mahmud, S., & Robal, M. (2012). Antimicrobial, rheological, and physicochemical properties of sago starch films filled with nanorod-rich zinc oxide. *Journal of Food Engineering, 113*(4), 511–519.

Ninan, N., Muthiah, M., Park, I.-K., Elain, A., Thomas, S., & Grohens, Y. (2013). Pectin/carboxymethyl cellulose/microfibrillated cellulose composite scaffolds for tissue engineering. *Carbohydrate Polymers, 98*(1), 877–885.

Olusola, O., Sisanda, D., Freeman, N., Williams, K., & Peter, A. (2019). Development and size distribution of polystyrene/ZnO nanofillers. *Procedia Manufacturing, 30*, 194–199.

Oun, A. A., & Rhim, J.-W. (2017). Carrageenan-based hydrogels and films: Effect of ZnO and CuO nanoparticles on the physical, mechanical, and antimicrobial properties. *Food Hydrocolloids, 67*, 45–53.

Paisoonsin, S., Pornsunthorntawee, O., & Rujiravanit, R. (2013). Preparation and characterization of ZnO-deposited DBD plasma-treated PP packaging film with antibacterial activities. *Applied Surface Science, 273*, 824–835.

Pengfeng, L., Liangling, L., Wenyan, X., Lihong, F., & Min, N. (2018). Preparation and characterization of aminated hyaluronic acid/oxidized hydroxyethyl cellulose hydrogel. *Carbohydrate Polymers, 199*, 170–177.

Poole, C. P., & Owens, F. J. (2003). *Introduction to nanotechnology*. New York: John Wiley & Sons.
Raghunath, A., & Perumal, E. (2017). Metal oxide nanoparticles as antimicrobial agents: A promise for the future. *International Journal of Antimicrobial Agents, 49*(2), 137–152.
Roberto, S., & Luigi, B. (2014). Nanofilled Thermoplastic–Thermoplastic polymer blends. In T. Sabu, S. Robert, & C. Sarathchandran (Eds.). *Nanostructured polymer blends* (pp. 133–160). New York: William Andrew Publishing.
Sekiguchi, Y., Sawatari, C., & Kondo, T. (2003). A gelation mechanism depending on hydrogen bond formation in regioselectively substituted O-methylcelluloses. *Carbohydrate Polymers, 53*(2), 145–153.
Shiv, S., Long-Feng, W., & Jong-Whan, R. (2019). Effect of melanin nanoparticles on the mechanical, water vapor barrier, and antioxidant properties of gelatin-based films for food packaging application. *Food Packaging and Shelf Life, 21*, 100363.
Tabassum, N., & Khan, M. A. (2020). Modified atmosphere packaging of fresh-cut papaya using alginate based edible coating: Quality evaluation and shelf life study. *Scientia Horticulturae, 259*, 108853.
Tankhiwale, R., & Bajpai, S. K. (2012). Preparation, characterization and antibacterial applications of ZnO-nanoparticles coated polyethylene films for food packaging. *Colloids and Surfaces B, Biointerfaces, 90*, 16–20.
Tingting, W., Jinqing, W., Rui, W., Peilin, Y., Zengjie, F., & Shengrong, Y. (2019). Preparation and properties of ZnO/sodium alginate bi-layered hydrogel films as novel wound dressings. *New Journal of Chemistry, 43*, 8684.
Thi, M. P., Thi, M. Q., Thi, X. T., & Pornchai, R. (2018). Effects of zinc oxide nanoparticles on the properties of pectin/alginate edible films. *International Journal of Polymer Science, 2018*, 5645797.
van der Linden, H. J., Herber, S., Olthuis, W., & Bergveld, P. (2003). Stimulus-sensitive hydrogels and their applications in chemical (micro)analysis. *Analyst, 128*(4), 325–331.
Vieira, J. G., Oliveira, G. D. C., Filho, G. R., Assunção, R. M. N. D., Meireles, C. D. S., Cerqueira, D. A., et al. (2009). Production, characterization and evaluation of methylcellulose from sugarcane bagasse for applications as viscosity enhancing admixture for cement based material. *Carbohydrate Polymers, 78*(4), 779–783.
Wang, J., Liu, H., Zhao, J., Gao, H., Zhou, L., Liu, Z., et al. (2010). Antimicrobial and antioxidant activities of the root bark essential oil of Periploca sepium and its main component 2-hydroxy-4-methoxybenzaldehyde. *Molecules, 15*(8), 5807–5817.
Wang, K., Lim, P. N., Tong, S. Y., & Thian, E. S. (2019). Development of grapefruit seed extract-loaded poly(ε-caprolactone)/chitosan films for antimicrobial food packaging. *Food Packaging and Shelf Life, 22*, 100396.
Wang, X.-Y., Luo, J.-P., Chen, R., Zha, X.-Q., & Pan, L.-H. (2015). Dendrobium huoshanense polysaccharide prevents ethanol-induced liver injury in mice by metabolomic analysis. *International Journal of Biological Macromolecules, 78*, 354–362.
Xie, L., Shen, M., Hong, Y., Ye, H., Huang, L., & Xie, J. (2020). Chemical modifications of polysaccharides and their anti-tumor activities. *Carbohydrate Polymers, 229*, 115436.
Yang, G., Zhang, L., Peng, T., & Zhong, W. (2000). Effects of Ca^{2+} bridge cross-linking on structure and pervaporation of cellulose/alginate blend membranes. *Journal of Membrane Science, 175*(1), 53–60.
Yoksan, R., & Chirachanchai, S. (2010). Silver nanoparticle-loaded chitosan–Starch based films: Fabrication and evaluation of tensile, barrier and antimicrobial properties. *Materials Science and Engineering C, 30*, 891–897.
Yu, J., Yang, J., Liu, B., & Ma, X. (2009). Preparation and characterization of glycerol plasticized-pea starch/ZnO–carboxymethylcellulose sodium nanocomposites. *Bioresource Technology, 100*(11), 2832–2841.
Yu, Y., Shen, M., Song, Q., & Xie, J. (2018). Biological activities and pharmaceutical applications of polysaccharide from natural resources: A review. *Carbohydrate Polymers, 183*, 91–101.
Zeng, P., Li, J., Chen, Y., & Zhang, L. (2019). The structures and biological functions of polysaccharides from traditional Chinese herbs. In L. Zhang (Ed.). *Progress in molecular biology and translational science* (pp. 423–444). Academic Press.
Zhang, L., Jiang, Y., Ding, Y., Daskalakis, N., Jeuken, L., Povey, M., et al. (2010). Mechanistic investigation into antibacterial behaviour of suspensions of ZnO nanoparticles against E. coli. *Journal of Nanoparticle Research, 12*(5), 1625–1636.
Zhang, Y., Pan, X., Ran, S., & Wang, K. (2019). Purification, structural elucidation and anti-inflammatory activity in vitro of polysaccharides from Smilax china L. *International Journal of Biological Macromolecules, 139*, 233–243.
Zulkifli, F. H., Hussain, F. S. J., Zeyohannes, S. S., Rasad, M. S. B. A., & Yusuff, M. M. (2017). A facile synthesis method of hydroxyethyl cellulose-silver nanoparticle scaffolds for skin tissue engineering applications. *Materials Science and Engineering C, 79*, 151–160.